A Comparative Study of Fractional Step Method in its Quasi-Implicit, Semi-Implicit and Fully-Explicit Forms for Incompressible Flows

Rhodri L.T. Bevan*, Etienne Boileau, Raoul van Loon and Perumal Nithiarasu†
Zienkiewicz Centre for Computational Engineering
College of Engineering, Swansea University
Singleton Park, Swansea SA2 8PP, UK

Abstract: The present review describes and analyses a class of finite element fractional step methods for solving the incompressible Navier-Stokes equations. Our objective is not to reproduce the extensive contributions on the subject, but to report on our long-term experience with and provide a unified overview of a particular approach: the characteristic based split method. Three procedures, the semi-implicit, quasi-implicit and fully-explicit, are studied and compared. This work provides a thorough assessment of the accuracy and efficiency of these schemes, both for a first and second order pressure split. In transient problems, the quasi-implicit form significantly outperforms the fully-explicit approach. The second order (pressure) fractional step method displays significant convergence and accuracy benefits when the quasi-implicit projection method is employed. The fully-explicit method, utilising artificial compressibility and a pseudo time stepping procedure, requires no second order fractional split to achieve second order or higher accuracy. While the fully-explicit form is efficient for steady state problems, due to its ability to handle local time stepping, the quasi-implicit is the best choice for transient flow calculations with time independent boundary conditions. The semi-implicit form, with its stability restrictions, is the least favoured of all the three forms for incompressible flow calculations.

1 Introduction

Fractional-step approximations to the incompressible Navier-Stokes equations comprise various projection-type methods developed under seemingly disparate formulations: projection onto a space of solenoidal vector fields (Temam 1977), pressure- or velocity-correction projection methods (van Kan 1986, Guermond & Shen 2003*b*), approximate matrix factorizations (Dukovicz & Dvinsky 1992, Perot 1993, Burton & Eaton 2002) or consistent splitting schemes (Guermond & Shen 2003*a*). Since the original work of Chorin (Chorin 1968, 1969) and Temam (Temam n.d.), this has developed into a widely employed procedure within the fields of aerospace, hydrodynamics and biomedical engineering (Kim & Moin 1985, Gresho et al. 1987, deSampaio et al. 1992, Drikakis et al. 1994, Bevan et al. 2010, Shen 1992, Nithiarasu et al. 2008, Bevan et al. 2011). The common denominator of these methods is the uncoupling of the momentum equations, which would otherwise have to be implicitly updated for incompressibility to be satisfied. When the projection method is combined with convection stabilization, introduced using higher order time stepping, the approach is typically referred to as the characteristic based split (CBS) scheme (Zienkiewicz & Codina 1995, Zienkiewicz et al. 1995, Codina et al. 1998, 2006, Nithiarasu & O.C.Zienkiewicz 2000, Nithiarasu et al. 2004, Arpino et al. 2010, Nithiarasu 2004, Morandi-Cecchi & Venturin 2006, Nithiarasu et al. 2006, Li & Duan 2006, Thomas et al. 2008). Variations within the CBS scheme are designated as the semi-implicit, quasi-implicit and fully-explicit

*Current address: Department of Aerospace Engineering, Faculty of Engineering, University of Bristol, Queen's Building, University Walk, Bristol BS8 1TR, UK
†Corresponding Author, e-mail: P.Nithiarasu@swansea.ac.uk

forms (Zienkiewicz et al. 2005, Nithiarasu et al. 2006), with reference to the pressure solution procedure. Hence in both the semi- and quasi-implicit forms, the momentum equations are treated entirely or partially explicitly. The fully-explicit scheme is in fact an iterative procedure providing an implicit approximation for the pressure, and is thus not a projection as such. A non-projection variant is also proposed for the quasi-implicit scheme. While all the three forms of the solution procedure have been adopted widely, a 'cross-method assessment' within the CBS family has yet to be fully addressed. In this work, the semi-, quasi-implicit and fully-explicit forms of the CBS scheme are brought together for the assessment of both steady-state and transient, laminar problems.

The loss of temporal accuracy due to the error resulting from the split has been the subject of a large number of articles (Perot 1993, Strikwerda & Lee 2000, Brown et al. 2001, Armfield & Street 2002), and much has been written about the boundary conditions to impose at each step (Kim & Moin 1985, Gresho et al. 1987, Temam 1991, Blasco et al. 1998, Lee et al. 2001, Nithiarasu 2002, Zienkiewicz et al. 2005). Hence we only discuss briefly some of these major aspects, mostly with reference to the CBS scheme. We also consider the role of the convective stabilization, the effect of using lumped or consistent mass matrices, and the computational efficiency of the scheme in its various forms.

Fractional step methods suffer from an inherent loss of temporal accuracy, due to the time splitting (or matrix factorisation in the fully discrete case), but this is usually considered negligible in comparison to the gain in computational efficiency. The location and impact of the splitting error is dependent upon the approach taken (Chang et al. 2002*a*) and whether such splitting induces changes to the momentum equations or to the incompressibility constraint. It is in fact well known that classical projection methods introduce a first order pressure error in time, when the pressure is completely removed at the fractional split stage (see *i.e.* (Codina 2001), and references therein). If the pressure is only partly removed, this introduces a known pressure instability, which may nevertheless be overcome using extra stabilization. This can be achieved by introducing the difference between the fully discrete and semi-discrete forms of the Navier-Stokes equations (Codina 2001). This method, originally developed for quasi-implicit methods, has since been applied to the fully-explicit CBS scheme (Nithiarasu & Zienkiewicz 2006), but the conclusions are not supported by convergence and accuracy studies. These aspects will be studied in the numerical experiments presented below.

The CBS scheme is typically derived in time, before any spatial discretization is performed (Zienkiewicz & Codina 1995, Zienkiewicz et al. 2005). Boundary conditions have to be imposed so that the intermediate semi-discrete problem is well-posed, which is not the case if the scheme is derived as a matrix decomposition (see (Perot 1993), for instance). In most projection methods, the normal component of the velocity is typically prescribed in the incompressibility step, but some approaches allow the enforcement of Dirichlet conditions on the velocity in all substeps (Blasco et al. 1998). Although it seems reasonable to assume that Dirichlet conditions should only be applied on the actual velocity field, rather than on the intermediate field(Kim & Moin 1985), this has its own drawbacks if the intermediate step involves natural boundary conditions. When using linear elements, the natural boundary conditions can result in a wrong approximation of the boundary tractions (Nithiarasu 2002). In applications in which the pressure gradient is approximately equal to zero, applying natural boundary conditions at the split stage can even be counter productive, in comparison to the Dirichlet boundary conditions. This will be demonstrated later via two transient examples. In addition, the impact of approximating the discrete operators, and the comparison of transient accuracy with and without lumped mass matrices, will be presented.

Convection stabilization is usually derived via a Taylor expansion (Zienkiewicz et al. 2005, Nithiarasu et al. 2006). Although this stabilization term may be essential for the fully-explicit method, to avoid oscillations at high Reynolds numbers, its importance is unclear for non-explicit schemes. The interest here is to identify the 'over diffusive' effects of those extra terms, which are a function of the time step.

The semi- and quasi-implicit approaches rely on a solution to the Poisson equation to determine the pressure field. The fully-explicit approach uses an artificial compressibility parameter (Nithiarasu 2003, Arpino et al. 2010) and a dual time stepping approach to achieve transient solutions. The rapidity of all schemes in determining an accurate solution is one of the critical characteristics of the schemes that requires assessment. The implementation has a very strong impact on the computational cost analysis. Therefore,

this work seeks to fully address these issues together in this paper. The first order pressure fractional step semi-implicit and fully-explicit methods have been previously compared (Massarotti et al. 2006), although the analysis concentrates on the time step (local and global), as applied to steady state problems. We now know that application of local time stepping to semi-implicit scheme produces adverse impact on the solution accuracy. Thus, the preliminary comparison reported between the explicit and semi-implicit schemes may not be completely valid. In addition to comparing the computational efficiency of the explicit and semi-implicit schemes, we also present the computational efficiency of both variants of the quasi-implicit scheme. The computational efficiency of these schemes are assessed in a relative sense for different combination of variations.

The rest of the paper is organised as follows. Section 2 presents the governing equations and a description of the first order pressure projection method, together with subsections outlining the three principal versions of the CBS scheme. In Section 3, the implementation of the second order pressure fractional step is presented. Section 4 details the solution strategy, and discuss some of the issues mentioned earlier, with reference to the CBS scheme. In Sections 5 to 7, three classical benchmark problems are presented, and conclusions are drawn in the last section.

2 Governing Equations and Numerical Methods

The non-conservative incompressible Navier-Stokes equations may be written in primitive variables as

$$\frac{\partial u_i}{\partial t} = -u_j \frac{\partial u_i}{\partial x_j} - \frac{\partial p}{\partial x_i} + \frac{1}{Re}\frac{\partial^2 u_i}{\partial x_j^2} \tag{1}$$

$$\frac{\partial u_i}{\partial x_i} = 0 \tag{2}$$

The equations are dimensionless with Re being the Reynolds number, u and p denote the dimensionless velocity and pressure respectively, which depend on space and time. The problem is completed by the specification of appropriate initial and boundary conditions. In its semi-discrete form, Eqn. (1) can be rewritten as

$$\frac{u_i^{n+1} - u_i^n}{\Delta t} = -u_j^{n+\theta_1} \frac{\partial u_i^{n+\theta_1}}{\partial x_j} - \frac{\partial p^{n+\theta_2}}{\partial x_i} + \frac{1}{Re}\frac{\partial^2 u_i^{n+\theta_3}}{\partial x_j^2} \tag{3}$$

where θ_i determines the time level at which each term is considered. The approximation of the non-linear terms may take other forms, but we only consider convection explicitly, *i.e* $\theta_1 = 0$ for all three schemes. The projection method operates as a two-stage fractional step scheme, based on a Helmholtz-Hodge decomposition. In the original method, the velocity is forced to satisfy a discrete divergence constraint at the end of each step, whereas this is not true for approximate pressure Poisson-type methods, such as the ones described in this article. In addition, as explained below, in the fully-explicit form the velocity is not projected onto a divergence-free subspace. All three forms of the CBS scheme can be derived using the auxiliary variables Δu_i^* and Δu_i^{**}, representing the split of Eqn. (3) into two parts

$$u_i^{n+1} - u_i^n = \Delta u_i^* + \Delta u_i^{**} \tag{4}$$

$$\frac{\Delta u_i^*}{\Delta t} = -u_j^{n+\theta_1} \frac{\partial u_i^{n+\theta_1}}{\partial x_j} + \frac{1}{Re}\frac{\partial^2 u_i^{n+\theta_3}}{\partial x_j^2} \tag{5}$$

$$\frac{\Delta u_i^{**}}{\Delta t} = -\frac{\partial p^{n+\theta_2}}{\partial x_i} \tag{6}$$

Taking the divergence of Eqn. (6) and expanding the semi-discrete form of the continuity Eqn. (2) at time level $n + \theta_4$ yields

$$\Delta t\theta_4\theta_2 \frac{\partial^2 \Delta p}{\partial x_i^2} = \frac{\partial u_i^n}{\partial x_i} + \theta_4 \frac{\partial \Delta u_i^*}{\partial x_i} - \Delta t\theta_4 \frac{\partial^2 p^n}{\partial x_i^2} \tag{7}$$

The method then consist in determining the initial auxiliary variable Δu_i^* using Eqn. (5), the pressure at t^{n+1} using Eqn. (7), and establishing the values of the velocity variables at level $n+1$ by obtaining the second auxiliary variable Δu_i^{**} using Eqn. (6).

Remark 2.1. The method outlined in this section does not fully represent the CBS scheme as convective stabilisation has not been included. The convective stabilisation may be recovered through a Taylor expansion, see Section 4.2.

Remark 2.2. The pressure-free projection method introduces a first order pressure error in the momentum equations. The fact that u^* is no longer within $O\left(\Delta t^2\right)$ of u^{n+1} also implies that a non-trivial approximation of the gradient term in Eqn. (6) is required when applying the boundary conditions at the intermediate steps. Approximating the updated pressure with p^n is sufficient and necessary to obtain second order accuracy in velocity (see (Kim & Moin 1985, Brown et al. 2001), for instance).

Remark 2.3. All three forms of the CBS scheme allow for equal order interpolation. The fractional step employing the pressure Poisson equation in the projection step result in a positive semi-definite matrix and a non-singular system for any choice of interpolation functions (see (Zienkiewicz et al. 2005, Codina & Blasco 1997), for instance).

The parameters θ_2 to θ_4 in the above equations have yet to be defined. Their choice determines the class variant and hence the appropriate strategy required to achieve a solution. However, $\frac{1}{2} \leq \theta_4 \leq 1$ remains consistent across the schemes detailed in the following subsections. The choice of the remaining parameters and hence the class variant is now introduced.

2.1 The Semi-Implicit Method

In the semi-implicit variant of the projection scheme, $1/2 \leq \theta_2 \leq 1$, and the discrete solution of Eqn. (7) involves a matrix inversion. The momentum equations are determined explicitly, with $\theta_3 = 0$. The fully discrete matrix form of the semi-implicit method (without convection stabilisation) may be written as
Step 1

$$\boldsymbol{M}\boldsymbol{\Delta u}^* = -\Delta t\boldsymbol{C}\boldsymbol{u}^n - \Delta t\boldsymbol{K}\boldsymbol{u}^n + \Delta t\boldsymbol{F}^n \tag{8}$$

where $\boldsymbol{M}$, $\boldsymbol{C}$ and $\boldsymbol{K}$ represent the mass matrix, discrete convection and viscous operators. $\boldsymbol{F}$ denotes the viscous boundary integral.
Step 2

$$\theta_2\theta_4\boldsymbol{L}\Delta p = \frac{1}{\Delta t}\left(\boldsymbol{D}\boldsymbol{u}^n + \theta_4\boldsymbol{D}\boldsymbol{\Delta u}^* - \theta_4\Delta t\boldsymbol{L}\Delta p\right) \tag{9}$$

Step 3

$$\boldsymbol{M}\boldsymbol{\Delta u} = \boldsymbol{M}\boldsymbol{\Delta u}^* - \Delta t\boldsymbol{G}\left(p^n + \theta_2\Delta p\right) \tag{10}$$

where $\boldsymbol{L}$, $\boldsymbol{D}$ and $\boldsymbol{G}$ represent the discrete Laplacian, divergence and gradient respectively. The semi-implicit scheme is conditionally stable, with the stability conditions arising from the convective and viscous terms respectively. The stability restrictions imposed on the scheme are defined as

$$\Delta t \leq \Delta t_{convective} = \frac{h}{\|\boldsymbol{u}\|} \tag{11}$$

and

$$\Delta t \leq \Delta t_{viscous} = \frac{h^2}{2Re} \tag{12}$$

where h is the element size. The viscous stability condition may impose a severe restriction on the time step allowed, negatively impacting the solution time of the problem. To overcome this, an alternative variant of the method may be employed. This is referred to as the quasi-implicit method.

2.2 The Quasi-Implicit Method

As opposed to the semi-implicit method, the quasi-implicit projection method treats the viscous term implicitly, $1/2 \leq \theta_3 \leq 1$. As $1/2 \leq \theta_2 \leq 1$, the terminology now refers to the momentum solution procedure, and the projection method is only nearly (quasi) implicit.

The first step of the quasi-implicit method is typically given as(Blasco et al. 1998)

$$(\boldsymbol{M} + \theta_3 \Delta t \boldsymbol{K})\, \boldsymbol{u}^* = \boldsymbol{M}\boldsymbol{u}^n - \Delta t \boldsymbol{C}\boldsymbol{u}^n + (\theta_3 - 1)\Delta t \boldsymbol{K}\boldsymbol{u}^n + \Delta t \boldsymbol{F}^n \tag{13}$$

with the boundary integral due to the viscous term still treated at time t^n. Steps 2 and 3 remain identical to the semi-implicit scheme, *i.e.* Eqn. (9) and Eqn. (10). A (non-projection) variant of the quasi-implicit form is obtained by discretizing the end-of-step velocity according to

$$(\boldsymbol{M} + \theta_3 \Delta t \boldsymbol{K})\, \boldsymbol{u}^{n+1} = \boldsymbol{M}\boldsymbol{u}^* - \Delta t \boldsymbol{G}\,(p^n + \theta_2 \Delta p) \tag{14}$$

In the later case, the scheme consist in solving Eqn. (13), Eqn. (9) and Eqn. (14). The time step restriction due to the stability limit is now only defined by

$$\Delta t \leq \Delta t_{convective} = \frac{h}{\|\boldsymbol{u}\|} \tag{15}$$

The quasi-implicit variant requires that simultaneous equations are solved for at least the first and second steps. While the computational time within each time step may be greater than that of the semi-implicit scheme, it may require only a reduced number of total time steps. The relative advantages of fewer time steps (quasi-implicit) versus fewer calculations per time step (semi-implicit) shall be quantified on the benchmark problem in Section 5.

2.3 The Fully Explicit Method

The artificial compressibility form of the CBS scheme has been employed since 2003 (Nithiarasu 2003). Being iterative, it provides an implicit approximation for the pressure. The continuity equation is re-written with an artificial wave speed parameter β

$$\frac{\partial \rho}{\partial t} = \frac{1}{\beta^2}\frac{\partial p}{\partial t} = -\frac{\partial(\rho u_i)}{\partial x_i} \tag{16}$$

Additionally, for the explicit procedure, $\theta_2 = 0$, and
Step 2

$$\left(\frac{1}{\beta^n}\right)^2 \boldsymbol{M}\Delta p = -\Delta t\,(\boldsymbol{D}\boldsymbol{u}^n + \theta_4 \boldsymbol{D}\boldsymbol{\Delta}\boldsymbol{u}^* - \Delta t \theta_4 \boldsymbol{L} p^n) \tag{17}$$

The first step within the projection method is identical to that of the semi-implicit method Eqn. (8). The use of the artificial compressibility requires that a pseudo iterative procedure be undertaken to calculate p^{n+1}. Thus, the Δt term refers in this case to a pseudo-time step within a pseudo iteration loop. To recover the true transient solution, an additional time stepping procedure (dual time stepping) must be employed. The transient solution is recovered through the modification of step 3 to include a true transient solution, *i.e.*,
Step 3

$$\boldsymbol{M}\boldsymbol{\Delta}\boldsymbol{u} = \boldsymbol{M}\boldsymbol{\Delta}\boldsymbol{u}^* - \Delta t \boldsymbol{G} p^n - \boldsymbol{M}_{\boldsymbol{\tau}} \frac{\boldsymbol{\Delta}\boldsymbol{u}_\tau}{\Delta \tau} \tag{18}$$

where $\Delta\tau$ is the true transient time step and $\boldsymbol{\Delta u}_\tau$ represents the change in the true transient velocities. This is approximated within this work by use of backward difference formulae (BDF). The first order BDF is defined as

$$\boldsymbol{\Delta u}_\tau = \boldsymbol{u}^n - \boldsymbol{u}^m \tag{19}$$

where m denotes the true transient time level and n denotes the pseudo time level. Additionally, the second and third order BDF are defined as

$$\boldsymbol{\Delta u}_\tau = \frac{3\boldsymbol{u}^n - 4\boldsymbol{u}^m + \boldsymbol{u}^{m-1}}{2} \tag{20}$$

and

$$\boldsymbol{\Delta u}_\tau = \frac{11\boldsymbol{u}^n - 18\boldsymbol{u}^m + 9\boldsymbol{u}^{m-1} - 2\boldsymbol{u}^{m-2}}{6} \tag{21}$$

respectively. The artificial compressibilty parameter β is locally determined based on both convective and diffusive stability restrictions (Nithiarasu 2003, Nithiarasu et al. 2004, Zienkiewicz et al. 2005) as well as the real time step size. This accommodates different flow regimes (either convection or diffusion dominated) locally within the domain. In this work the relation $\beta = \max(\epsilon, \nu_{conv}, \nu_{diff}, \nu_{real})$ is employed. The constant $0.1 \leq \epsilon \leq 1.0$ ensures that β does not approach zero. $\nu_{real} = h/\Delta\tau$, ν_{conv} is the local convective velocity and ν_{diff} is the local diffusive velocity. These velocities are calculated from the non-dimensional relations (Nithiarasu 2003),

$$\nu_{conv} = \sqrt{u_i u_i} \qquad \nu_{diff} = \frac{1}{hRe} \tag{22}$$

In the fully explicit method, no restriction is imposed on the true transient time step, although the stability criteria identified for the semi-implicit scheme do apply to the pseudo time step. If the mass matrix $\boldsymbol{M}$ is lumped, then the solution procedure is matrix free. This is easily done with linear elements.

3 Second Order Pressure Projection Methods

The pressure term may be partially reintroduced in the momentum equations

$$\frac{\Delta u_i^*}{\Delta t} = -u_j^{n+\theta_1}\frac{\partial u_i^{n+\theta_1}}{\partial x_j} + \frac{1}{Re}\frac{\partial^2 u_i^{n+\theta_3}}{\partial x_j^2} - \frac{\partial p^n}{\partial x_i} \tag{23}$$

with the correction becoming

$$\frac{\Delta u_i^{**}}{\Delta t} = -\theta_2\frac{\partial \Delta p}{\partial x_i} \tag{24}$$

The pressure is now determined by

$$\Delta t\theta_4\theta_2\frac{\partial^2 \Delta p}{\partial x_i^2} = \frac{\partial u_i^n}{\partial x_i} + \theta_4\frac{\partial \Delta u_i^*}{\partial x_i} \tag{25}$$

This second order pressure scheme does not retain the stabilising properties of the first order pressure projection method (Codina 2001). To overcome this penalty, it is necessary to include additional stabilisation. The fully discrete form of the correction step Eqn. (10), when rearranged and substituted into the fully discrete continuity equation, results in

$$\theta_4\Delta t^2\boldsymbol{D}\boldsymbol{M}^{-1}\boldsymbol{G}\left(p^n + \theta_2\Delta p\right) = \Delta t\boldsymbol{D}\boldsymbol{u}^n + \theta_4\Delta t\boldsymbol{D}\boldsymbol{\Delta u}^* \tag{26}$$

The Laplacian operator $\boldsymbol{L}$ appears as an approximation of $\boldsymbol{D}\boldsymbol{M}^{-1}\boldsymbol{G}$. This can also be derived with a block LU factorisation of the fully discretized equations, and using the approximation $\Delta t\boldsymbol{M}^{-1}$ to the inverse of the momentum system matrix. The difference between Eqn. (9) and Eqn. (26) is then employed as a method of increasing the stabilisation. An explicit treatment allows for rapid computation. This stabilisation approach requires the solution of an intermediate variable prior to calculation of the pressure field. This variable is determined by

$$\boldsymbol{M}\boldsymbol{Z}^n = \boldsymbol{G}p^n \tag{27}$$

It should be noted that $\boldsymbol{M}$ and $\boldsymbol{G}$ are evaluated over the entire domain (including the boundary). Although this has not been made clear in (Codina 2001) and (Nithiarasu & Zienkiewicz 2006), boundary conditions for velocity may be imposed on $\boldsymbol{Z}$, since the variable is derived from the correction step. Finally, the stabilised form of Eqn. (25) may be given as

$$\theta_2\theta_4(1+\gamma)\boldsymbol{L}\Delta p = \frac{1}{\Delta t}\left(\boldsymbol{D}\boldsymbol{u}^n + \theta_4\boldsymbol{D}\boldsymbol{\Delta}\boldsymbol{u}^* + \gamma\theta_4\Delta t\boldsymbol{D}\boldsymbol{Z}^n\right) \tag{28}$$

where γ represents the stabilisation parameter. Equation (28) is valid for the semi- and quasi-implicit schemes. For the variant of the later, Eqn. (27) may be modified as follows

$$\left(\boldsymbol{M} + \theta_3\Delta t\boldsymbol{K}\right)\boldsymbol{Z}^n = \boldsymbol{G}p^n \tag{29}$$

For the fully explicit scheme, the dual time stepping must be taken into account. Thus, Eqn. (27) becomes

$$\boldsymbol{M}\boldsymbol{Z}^m = \boldsymbol{G}p^m \tag{30}$$

and since the fully explicit $\boldsymbol{M}$ is lumped, the matrix free approach persists. This small calculation is performed once per real time step. Finally, the pressure step is given as

$$\left(\frac{1}{\beta^n}\right)^2 \boldsymbol{M}\Delta p = -\Delta t\left(\boldsymbol{D}\boldsymbol{u}^n + \theta_4\boldsymbol{D}\boldsymbol{\Delta}\boldsymbol{u}^*\right) + \Delta t^2\theta_4\boldsymbol{L}((1+\gamma)p^n - p^m) - \Delta t^2\gamma\theta_4\boldsymbol{D}\boldsymbol{Z}^m \tag{31}$$

4 Solution Strategy

Of the four methods outlined, including the variant to the quasi-implicit scheme, only the fully-explicit approach is matrix free. To solve the pressure step, a preconditioned conjugate gradient solver is employed, with a Jacobi or diagonal preconditioner for straightforward parallelisation.

4.1 Time Stepping

Stability criteria Eqn. (11), Eqn. (12), Eqn. (15) and Eqn. (22) depend on the element size h. The nodal value of h is calculated by taking the minimum value of the element sizes surrounding the node. On a non-uniform mesh, the element size will vary and hence the nodal time step. While local time stepping in the fully explicit case is clearly advantageous to accelerate convergence to the intermediate steady state, the case for local time stepping in the semi- and quasi-implicit methods is less clear. From (Massarotti et al. 2006) the use of local time stepping is clearly disadvantageous in the semi-implicit scheme, with the results showing serious discrepancies. In the quasi-implicit method, the use of local time stepping would produce non-symmetric matrices, precluding the use of symmetric solvers. While non-symmetric solvers may be employed, this has not been investigated in this paper. Therefore, for the semi-implicit and quasi-implicit methods, the global time step is determined from the minimum local time step. The final time step is then multiplied by a safety factor to ensure that it remains below the stability limit.

4.2 Convective Stabilisation

For most convection dominated flows, the explicit fractional step method will require some form of stabilization. This is especially true when the element Peclet number is much greater than unity. The scheme takes the form of an explicit characteristic-Galerkin procedure (Zienkiewicz et al. 2005, Zienkiewicz & Codina 1995, Zienkiewicz et al. 1995), and is written semi-discretely as

$$u_i^{n+1} - u_i^n = \Delta t \left(-u_j^{n+\theta_1} \frac{\partial u_i^{n+\theta_1}}{\partial x_j} - \frac{\partial p^{n+\theta_2}}{\partial x_i} + \frac{1}{Re} \frac{\partial^2 u_i^{n+\theta_3}}{\partial x_j^2} \right) + \frac{\Delta t^2}{2} u_k \frac{\partial}{\partial x_k} \left(-u_j^n \frac{\partial u_i^n}{\partial x_j} - \frac{\partial p^n}{\partial x_i} + \frac{1}{Re} \frac{\partial^2 u_i^n}{\partial x_j^2} \right) \tag{32}$$

While convective stabilisation is required within the fully-explicit method, its requirement within the semi- and quasi-implicit methods is questionable. Since the stabilization term is a function of the time step, the larger time steps employed by the semi- and quasi implicit schemes may result in over diffusive solution. This is examined in the first benchmark example.

4.3 Imposition of Velocity Boundary Conditions

The classical projection methods, including the CBS family, are derived using the semi-discrete form, *i.e.* the equations are split after being discretized in time only. The result is that the operators require appropriate boundary conditions, so that the intermediate semi-discrete problem is well-posed. On the contrary, if the split is interpreted as a matrix factorisation, the boundary conditions are incorporated in the fully discrete operators. Continuous and discrete operators do not have the same properties, and attempts to improve the time order accuracy though boundary conditions, or the pressure update scheme, have been the subject of much debate (van Kan 1986, Bell et al. 1989, Perot 1993, Blasco et al. 1998, Strikwerda & Lee 2000, Brown et al. 2001, Chang et al. 2002*b*, Armfield & Street 2002). An often disregarded detail in all these numerical experiments is the fact that in each case the computational domain or, more specifically, the use of periodic boundary conditions, will affect the temporal order of convergence of the method.

For the numerical examples presented below, imposition of natural boundary conditions for the intermediate problem will result in a loss of accuracy, due to an extra approximation (projection to boundaries) of the derivatives (Nithiarasu 2002). For problems in which the pressure gradient is zero at the boundary, imposition of such conditions can even be counterproductive. The use of Dirichelt conditions for the intermediate velocity shall be explored in Section 6.

5 First Benchmarck - Lid-Driven Cavity Flow

The first problem considered is that of the lid-driven cavity flow: no-slip conditions on the walls, top wall is allowed to move at a uniform horizontal velocity, the fluid within the cavity is initially at rest. The numerical experiments analyse *(a)* the impact of convection stabilization, *(b)* accuracy and *(c)* the speed of all the three principal variants of the projection scheme. The problem is solved on the meshes given in Fig.1, with $\theta_2 = 1$ for the semi- and quasi-implicit schemes, and $\theta_4 = 1$ for all three methods.

The semi-implicit method employs the lumped mass matrix at steps 1 and 3, the quasi-implicit projection method employs the lumped mass matrix at step 3 and the fully-explicit method employs the lumped mass matrix at all the three steps. The global time steps are employed for the semi- and quasi- implicit schemes and local time stepping is employed for the explicit scheme. The time step values are calculated according to the stability criteria discussed previously. A minimum global time step is then chosen for semi- and quasi-implicit schemes and multiplied by a safety factor (0.7 for the semi- and quasi-implicit, 0.4 for the fully-explicit).

The impact of convection stabilisation is studied and the results are presented in Fig. 2, for the quasi-implicit method. If the use of the characteristic-Galerkin procedure seems to have no apparent effect on the accuracy of both the semi-implicit and the fully-explicit schemes (not shown), it appears to be unnecessary

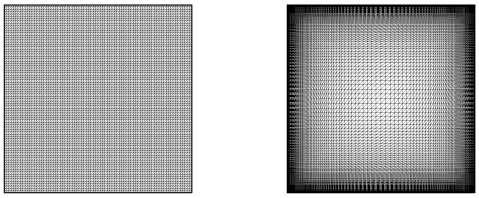

(a) (b)

Figure 1: Lid-driven cavity problem. a) Mesh A: uniform structured 12800 linear elements, b) Mesh B: non-uniform structured 28800 linear elements.

Table 1: Lid-driven cavity problem. Location of vortices given by the quasi-implicit projection method and their comparison with the simulation of Ghia *et al.* (Ghia et al. 1982).

		Primary Vortex		Bottom Right (first vortex)	
	Location	x	y	x	y
Re=100	Predicted	0.616	0.737	0.943	0.062
	Ghia *et al.*	0.617	0.734	0.945	0.063
Re=400	Predicted	0.555	0.606	0.886	0.123
	Ghia *et al.*	0.555	0.606	0.891	0.125
Re=3200	Predicted	0.518	0.541	0.824	0.084
	Ghia *et al.*	0.517	0.547	0.813	0.086

and disadvantageous for the quasi-implicit method, although this is minimised with the smaller time step employed for Mesh B ($Re = 400$). Consequently, the remaining results presented only include the stability component for the semi-implicit and fully-explicit approaches.

Table 1 reports the predicted location of vortices based upon the results of the quasi-implicit scheme. Stream traces and pressure distribution were calculated, as well as horizontal and vertical velocity cross-sections for all three schemes, and the results are in good agreement with each other and with those predicted by Ghia *et al.* (Ghia et al. 1982). The computational cost varies, however, as shown in Tab. 2. For this particular problem, only a single CPU (Intel QX9600) was employed to ensure the timing was not affected by parallel implementation. The steady state was said to have been achieved when the L2 norm of the velocity reduced to below 1.0×10^{-7}. The run times were determined via the MPI_WTIME call.

Examining the benchmark results for all Reynolds numbers, it is clear that the semi-implicit scheme does not provide any advantage over the quasi-implicit scheme. The fully-explicit scheme is only marginally faster at $Re = 400$ and is clearly a sub-optimal choice at $Re = 100$ and $Re = 3200$. Admittedly, these results are for a uniform structured mesh, and the global time step used in the quasi-implicit scheme is not heavily penalised by the existence of varying element sizes. For the higher resolution (and non-uniform structured, with ratio of largest to smallest element area of 365) Mesh B, the corresponding run times are given in Tab. 3. These were conducted on two quad core Intel Nehalem Xeon processors (3Ghz) within a small cluster. At $Re = 3200$, the value of the safety factor has a small impact on the accuracy of the fully-explicit solution. While a value of 0.4 was employed initially, this was reduced to 0.1 to achieve an accuracy comparable to that of the other two projection methods. Further, the choice of ϵ within the artificial parameter β was initially 0.5. To achieve a more rapid solution, this was increased to $\epsilon = 1.0$, and this change was made

Table 2: Lid-driven cavity problem. Run-time analysis using Mesh A.

	Re = 100		Re = 400		Re = 3200	
	time (s)	steps	time (s)	steps	time (s)	steps
Semi-Implicit	309.36	6049	309.92	5369	551.13	10240
Quasi-Implicit	177.86	2924	323.97	5384	519.03	10030
Fully Explicit	232.42	22460	305.28	28650	760.95	72400

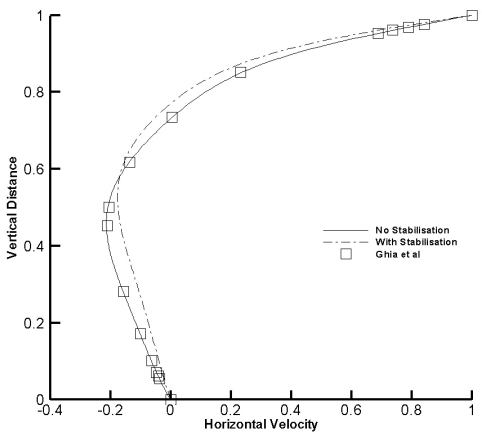

(a) Re=100

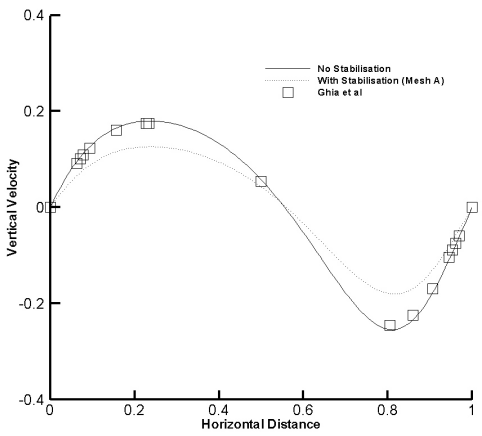

(b) Re=100

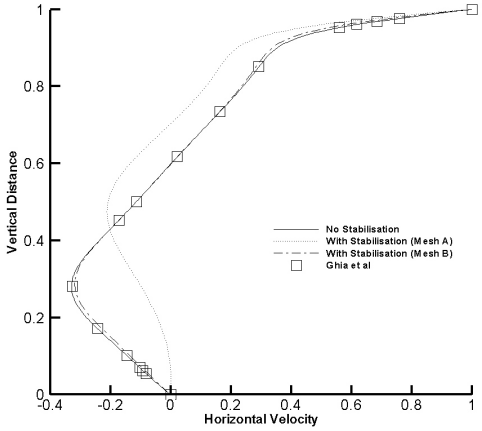

(c) Re=400

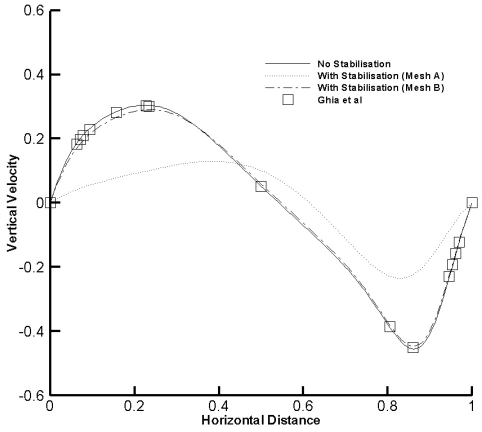

(d) Re=400

Figure 2: Lid-driven cavity problem. Impact of convection stabilisation on the accuracy for quasi-implicit projection method.

Table 3: Lid-driven cavity problem. Run-time analysis using Mesh B.

	Re = 400		Re = 1000		Re = 3200	
	time (s)	steps	time (s)	steps	time (s)	steps
Semi-Implicit	3984.83	186600	1963.26	89300	2892.26	137300
Quasi-Implicit	995.99	45200	1125.19	52700	2983.77	137600
Fully Explicit	101.82	45900	220.03	100500	1292.18	589600

for both meshes at $Re = 3200$. The impact of a non-uniform mesh is significant on both the semi- and quasi-implicit schemes, due to the use of a global time step.

All schemes provided near identical solutions to the benchmark problem presented. Their suitability for a particular numerical experiment must consider the computational cost and run time requirements. The semi-implicit form, with its diffusive stability restrictions, is the least favoured of all the three schemes, and this would be particularly true for problems involving meshes with stretched elements parallel to the flow (e.g. in a boundary layer region). The choice between the quasi-implicit scheme and the fully explicit projection method is currently less clear. While the quasi-implicit approach demonstrates a clear advantage for uniformly structured meshes, the reverse is true for non-uniform meshes. Further, the use of BDF for the real time step within the fully explicit scheme (which are not constrained by stability criteria) may provide an additional advantage during transient problems.

6 Second Benchmark - Analytical Problem of Vortex Decay

The second problem considered is that of vortex decay within a unit square domain. The two-dimensional unsteady flow problem is an analytical solution to the incompressible Navier-Stokes equations, defined as

$$\begin{aligned} u(x,y,t) &= -\cos \pi x \sin \pi y \exp^{-2\pi^2 t/Re} \\ v(x,y,t) &= \sin \pi x \cos \pi y \exp^{-2\pi^2 t/Re} \\ p(x,y,t) &= -\frac{1}{4}\left(\cos 2\pi x + \cos 2\pi y\right) \exp^{-4\pi^2 t/Re} \end{aligned} \tag{33}$$

The initial and boundary conditions are taken from the analytical solution. This problem quantitatively assesses the transient properties of the quasi-implicit and fully-explicit methods. The semi-implicit approach is not presented here, as it was found to be sub-optimal in the previous section. For the BDF in the fully-explicit method, the prior time step values are determined accordingly. A uniformly structured mesh of 28800 linear triangular elements is employed.

As outlined in Section 4.3, applying boundary conditions to both step 1 and step 3 is more accurate for this problem than imposing only step 3 boundary conditions for velocity for the quasi-implicit scheme (see Fig. 3). The L2 norm of the error relative to the analytical solution was determined at $t = 1$. The result presented are for a lumped mass matrix, with the $\boldsymbol{M} + \Delta t \boldsymbol{K}$ matrix used in the correction step. The use of boundary conditions is more accurate due to the appropriate pressure gradient being zero on the boundary. Thus, the correction is zero on the boundary and the intermediate velocity is the actual velocity field for the next step. This demonstrates that there is a small but appreciable error due to the diffusive natural boundary condition. The use of boundary conditions within step 1 produces no discernible impact upon the fully-explicit projection method, as expected.

Although the real time step term must be included within the initial step, if using the fully discretized matrix factorisation, it has been typically incorporated at the correction step (Nithiarasu 2003, Nithiarasu et al. 2004, Nithiarasu & Zienkiewicz 2006, Massarotti et al. 2006). In fact, if included within the initial step, it would reduce the correction required and the number of iterations within every real time step. Both alternatives were investigated using this benchmark problem, and the impact was found to be negligible. The real time step term was arbitrarily implemented within the correction step.

Figure 4 gives the convergence of the first order (velocity and pressure) quasi-implicit and fully-explicit schemes using both lumped and consistent mass matrices. A least squares technique was employed to calculate the rate of convergence, and the result is given in Tab. 4. The third column refers to the fractional step approach taken for the quasi-implicit scheme, and shows which matrix is employed within the correction step.

From Tab. 4, the fully-explicit displays a perfect first order convergence for both pressure and velocity. The quasi-implicit method also displays perfect convergence when the $\boldsymbol{M} + \Delta t \boldsymbol{K}$ matrix is employed within the correction step, as opposed to only $\boldsymbol{M}$ (whether in consistent or lumped form), which displays less than

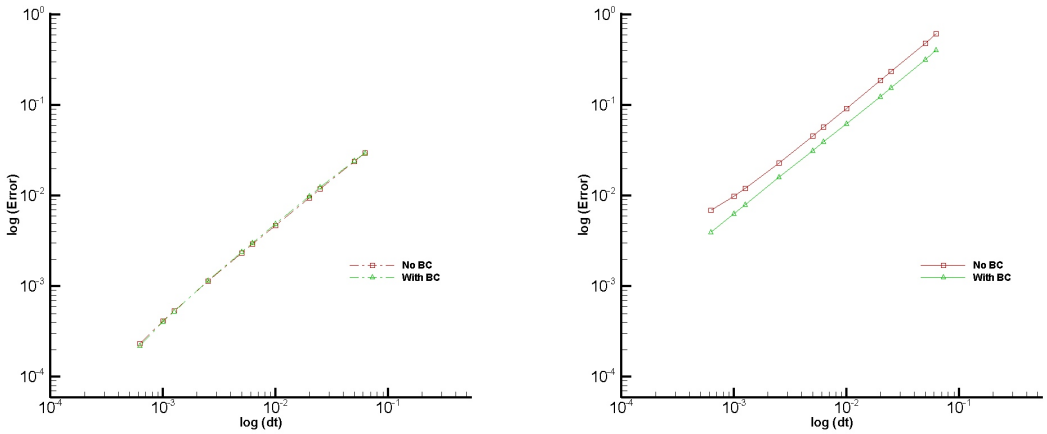

(a) velocity (b) pressure

Figure 3: Vortex decay. Influence on the rate of convergence of imposing step 1 boundary conditions for the quasi-implicit method.

Table 4: Vortex decay. Calculated rate of convergence for 1^{st} order velocity/1^{st} order pressure.

Method	Mass Matrix	Step 3	Velocity	Pressure
QI	Consistent	$\boldsymbol{M} + \Delta t \boldsymbol{K}$	1.053	1.001
QI	Consistent	$\boldsymbol{M}$	1.071	0.670
EX	Consistent	-	1.036	1.043
QI	Lumped	$\boldsymbol{M} + \Delta t \boldsymbol{K}$	0.982	0.985
QI	Lumped	$\boldsymbol{M}$	1.000	0.675
EX	Lumped	-	1.024	1.030

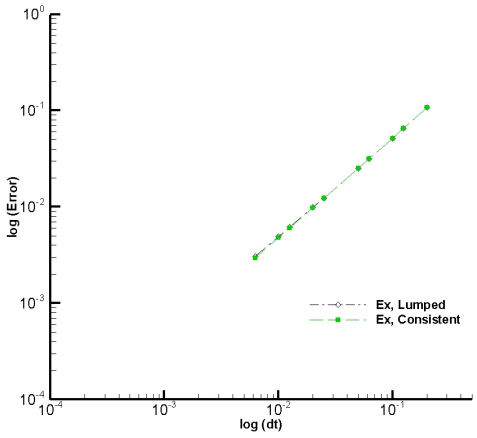

(a) EX, velocity

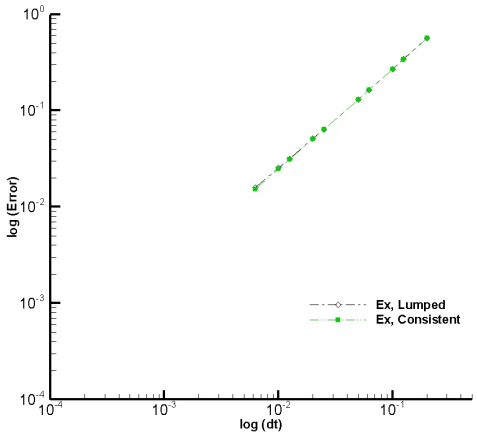

(b) EX, pressure

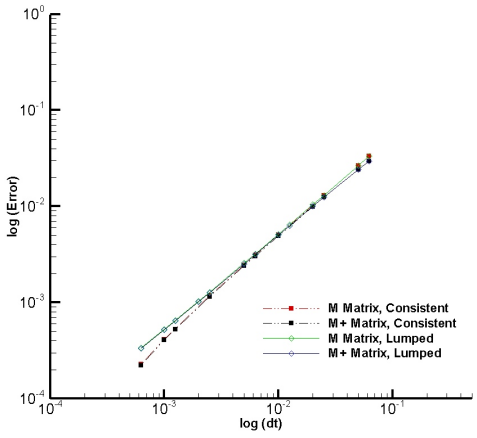

(c) QI, velocity

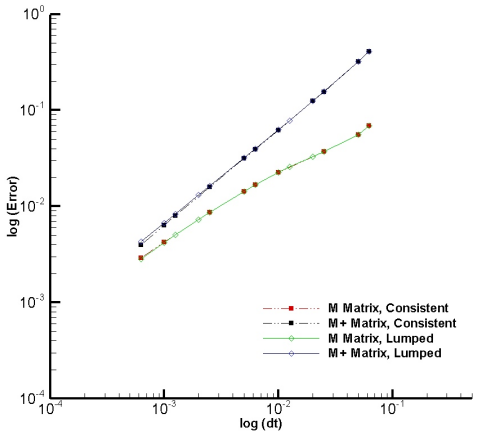

(d) QI, pressure

Figure 4: Vortex decay. Convergence results for 1^{st} order velocity/1^{st} order pressure.

Table 5: Vortex decay. Calculated rate of convergence for 2^{nd} order velocity/1^{st} order pressure.

Method	Mass Matrix	Step 3	Velocity	Pressure
QI	Consistent	$\boldsymbol{M} + \Delta t \boldsymbol{K}$	1.274	0.833
QI	Consistent	$\boldsymbol{M}$	1.328	0.811
EX	Consistent	-	2.060	2.039
QI	Lumped	$\boldsymbol{M} + \Delta t \boldsymbol{K}$	1.614	0.808
QI	Lumped	$\boldsymbol{M}$	1.847	0.848
EX	Lumped	-	2.174	1.944

first order pressure convergence. The convergence information in the figures is complicated by the error displayed for a given time step. The $\boldsymbol{M} + \Delta t \boldsymbol{K}$ matrix quasi-implicit scenarios contain a greater error at each time level, and this is due to the fractional split error allocation. When the identity matrix is used in step 2 (see Eqn. (26), where the approximation to the inverse system matrix is now only given by the Laplacian, *i.e.* $\boldsymbol{M}^{-1} = \boldsymbol{I}$ in this case), all the split error is contained within the incompressibility constraint.

A second order velocity procedure improves the rate of convergence, but the scheme remains first order for pressure. A second order BDF is employed for the fully-explicit method. The relevant prior values of the velocity are determined from the analytical solution. In the quasi-implicit scheme, $\theta_3 = 0.5$ (Crank-Nicholson), and a second order Adams-Bashforth scheme was used for the convection component. The results are presented in Tab. 5 and Fig 5. The fully-explicit method demonstrates second order convergence of both pressure and velocity. The second order convergence of the pressure is due to the pseudo timestepping iteration procedure within the fully-explicit method. The use of an Adams-Bashforth linear multistep method, rather than Euler was investigated within the iteration loop of the fully-explicit method. This had virtually no impact on either the accuracy or the number of iterations required. Both variants of the quasi-implicit method display varying rates of convergence. Indeed, the $\boldsymbol{M}$ scenarios show a varying rate of convergence, depending on the magnitude of the time step. This is potentially due to the Laplacian approximation within step 2, as mentioned earlier. As the time step is reduced, the impact of this approximation is also reduced (due to the Δt^2 in Eqn. (26)). The lumped $\boldsymbol{M}$ variant displays a smaller error than the equivalent consistent approach, due to a minimising of the error contained within the incompressibility constraint. The error is shared between the incompressibility constraint and the momentum equations with the consistent mass matrix. With the $\boldsymbol{M} + \Delta t \boldsymbol{K}$ quasi-implicit scenarios, the error is contained within the incompressibility constraint, rather than the momentum. This results in a smaller error for a given time step. Since the error is contained within the pressure equation, the first order pressure convergence appears to have a greater influence on the convergence rate of the velocity compared to the $\boldsymbol{M}$ approach. It is noteworthy that the lumped $\boldsymbol{M} + \Delta t \boldsymbol{K}$ quasi-implicit scheme demonstrates near identical values of the L2 norm of the velocity error, to that of the fully-explicit method, for the region of overlap.

From Tab. 5, it is clear that the quasi-implicit scheme is not displaying second order convergence for the velocity. This may be partly due to the pressure convergence. Therefore, it is necessary to assess the impact of employing the second order pressure projection method outlined in Section 3. As the fully explicit method has already demonstrated second order convergence (pressure and velocity), it is expected that this will have minimal impact for this scheme. The value of the stability parameter γ is taken as 0.25 (Nithiarasu & Zienkiewicz 2006, Codina 2001). No boundary conditions are imposed for the intermediate variable $\boldsymbol{Z}$.

To demonstrate the necessity of the additional stability within the pressure determination, Fig. 6 gives the pressure and velocity contours with and without the stability term. The stabilisation provides sufficient smoothing to recover an accurate pressure field. The distributions of the velocity are unaffected, and both simulations produce an identical solution. The fully-explicit method does not display any oscillations for the pressure field when the additional stabilisation is absent, and this is due to the scheme employing artificial compressibility as an iterative mechanism.

The results from the fully-explicit and quasi-implicit second order pressure methods are presented in Tab. 6 and Fig. 7. For the convergence results presented in this section, the lumped mass matrix provides an optimal solution, compared to that of the consistent mass matrix. This applies to both the overall error at a particular time step and to the convergence. When using a consistent mass matrix, the rate of convergence tends to decrease with a reduced time step. This is particularly true for the velocity convergence (likely due

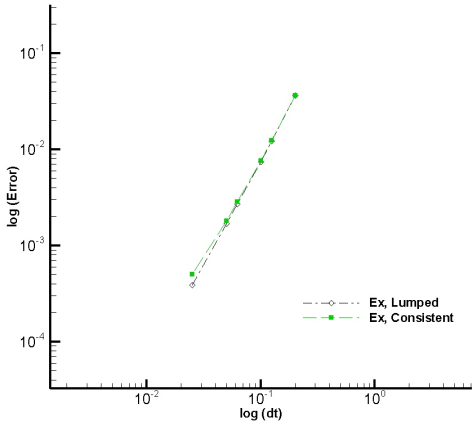

(a) EX, velocity

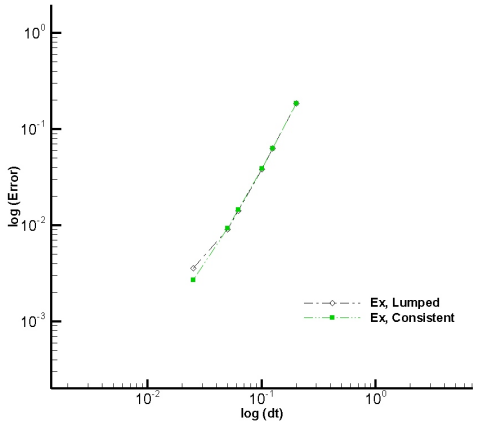

(b) EX, pressure

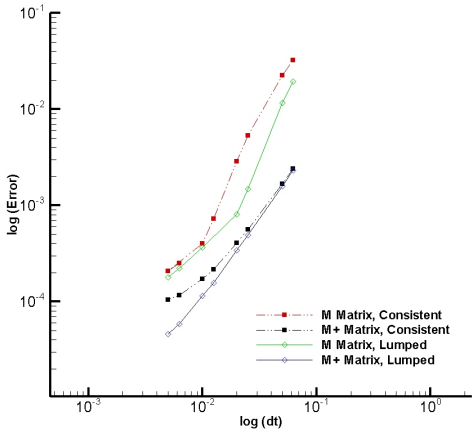

(c) QI, velocity

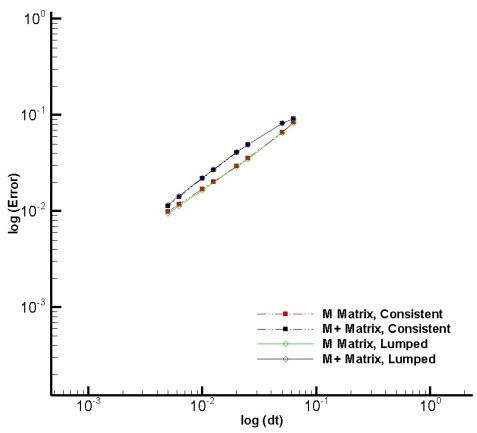

(d) QI, pressure

Figure 5: Vortex decay. Convergence results for 2^{nd} order velocity/1^{st} order pressure.

Table 6: Vortex decay. Calculated rate of convergence for 2^{nd} order velocity/2^{nd} order pressure.

Method	Mass Matrix	Step 3	Velocity	Pressure
QI	Consistent	$\boldsymbol{M} + \Delta t \boldsymbol{K}$	3.086	1.706
QI	Consistent	$\boldsymbol{M}$	2.811	1.656
EX	Consistent	-	2.103	2.082
QI	Lumped	$\boldsymbol{M} + \Delta t \boldsymbol{K}$	3.709	1.704
QI	Lumped	$\boldsymbol{M}$	2.270	1.671
EX	Lumped	-	2.197	2.067

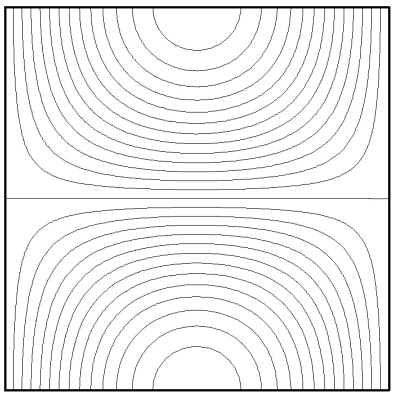

(a) u

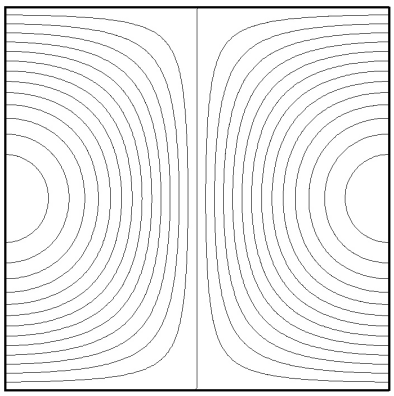

(b) v

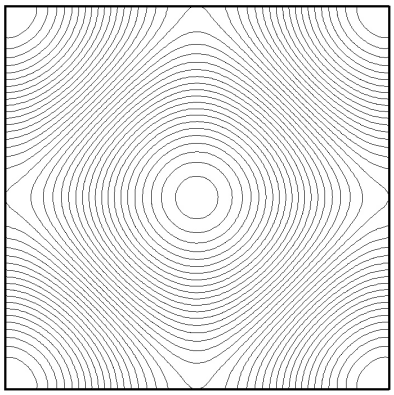

(c) QI, p, $\gamma = 0.25$

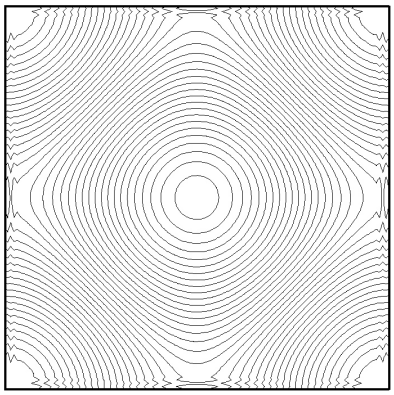

(d) QI, p, $\gamma = 0.00$

Figure 6: Vortex decay. Necessity of additional pressure stability for 2^{nd} order pressure projection method.

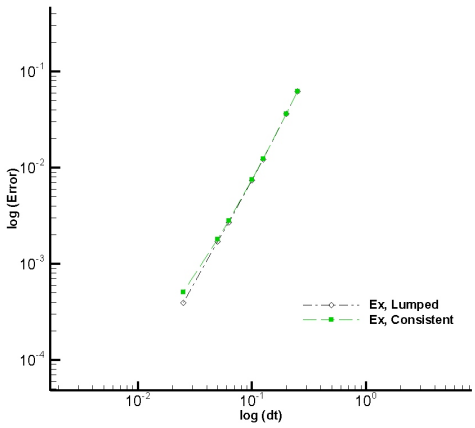

(a) EX, velocity

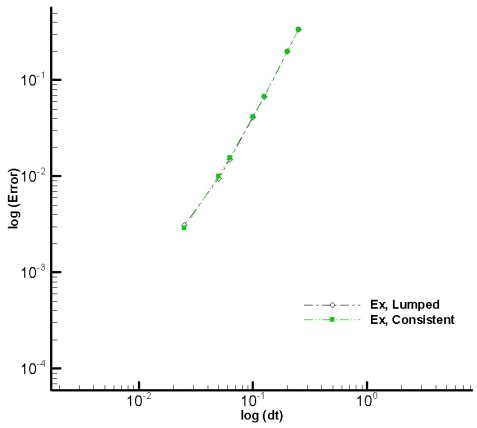

(b) EX, pressure

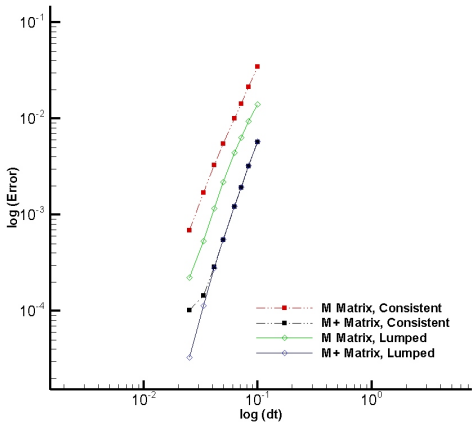

(c) QI, velocity

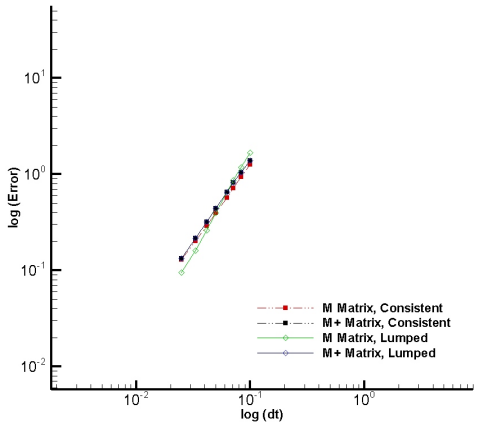

(d) QI, pressure

Figure 7: Vortex decay. Convergence for 2^{nd} order velocity/2^{nd} order pressure.

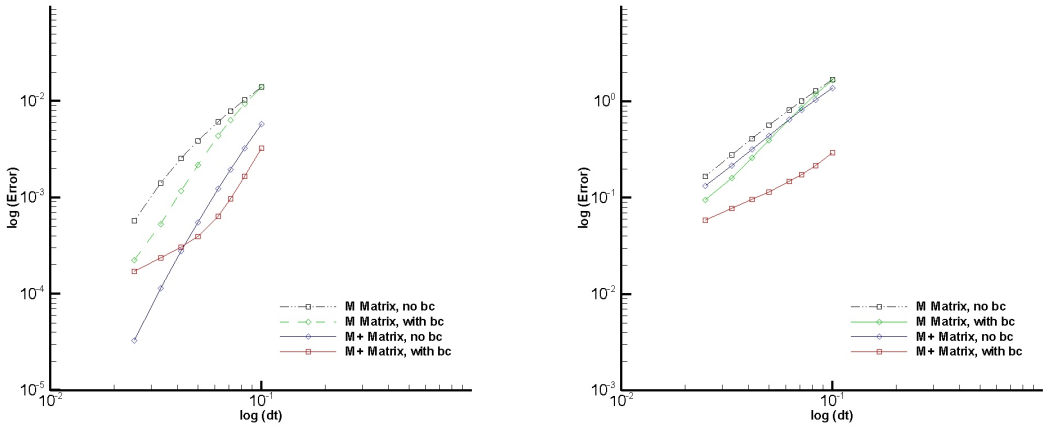

(a) velocity

(b) pressure

Figure 8: Vortex decay. Impact of boundary conditions upon the stability intermediate variable $\boldsymbol{Z}$ and convergence.

to the order of magnitude difference between the pressure and velocity error), and for both the fully-explicit and quasi-implicit results. The mass matrix is thus preferentially lumped in this case.

The fully-explicit method experiences only a minor improvement in the convergence of both velocity and pressure, as compared to the second order velocity/first order pressure. The quasi-implicit method displays a significant improvement in the convergence of both pressure and velocity. According to the results, the quasi-implicit scheme is demonstrating greater than second order convergence for the velocity, in all four scenarios. It is necessary to note that the calculated gradient is dependent on small log scale differences, which provides a degree of inaccuracy in the least squares calculation. The discrepancy is nevertheless significantly above this threshold. If velocity boundary conditions are now imposed for the intermediate variable $\boldsymbol{Z}$, then the convergence is likely to be influenced.

The impact of velocity boundary conditions is displayed graphically in Fig. 8 for a lumped mass matrix. Results with $\boldsymbol{M}$ alone demonstrate an improved velocity and pressure convergence when the boundary conditions are employed. The rate of convergence for velocity and pressure increase from 2.270 to 3.068 and 1.671 to 2.111 respectively. Whereas results show that when $\boldsymbol{M} + \Delta t \boldsymbol{K}$ is used, a decrease in the convergence rates of both velocity and pressure is experienced. The velocity rate of convergence decreases from 3.710 to 2.068, and the pressure convergence from 1.704 to 1.129. This negative influence is likely due to the introduction of numerical boundary layers within the pressure field. From these results, imposition of boundary conditions seems to be beneficial for the $\boldsymbol{M}$ case, but should not be employed when the diffusive component is included within the matrix of the correction step. The impact on mass imbalance shall be assessed in the final benchmark.

The rate of convergence for the fully-explicit method is given in Tab. 7 and Fig. 9, when a third order BDF is used. As expected, the order of BDF determines the rate of convergence for both velocity and pressure. The second order pressure fractional split has only a very small improvement over the classical fractional split, while requiring a near identical number of iterations. As such, the second order fractional split is sub-optimal, compared to the classical fractional split, mostly due to the increased number of calculations required. The rate of convergence has been determined from only six points, due to the rapid nature of convergence. Indeed, for the smaller timesteps, the maximum nodal error in both the velocity and the pressure is of the order 10^{-5}. This explains the higher than expected error in the rate of convergence. To reduce the error, it was necessary to provide a low iteration convergence tolerance within the pseudo timestepping loop, as demonstrated in Tab. 8. The fully-explicit scheme utilised two tolerance checks to

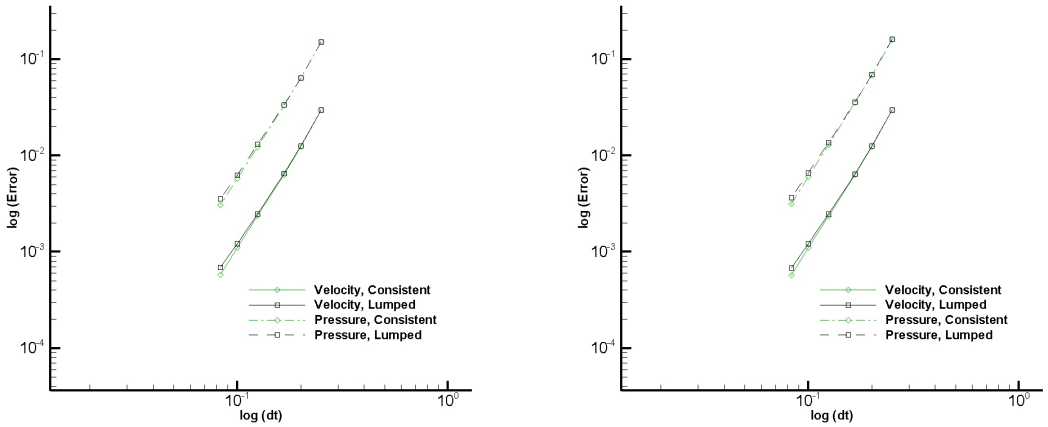

(a) 1^{st} order pressure

(b) 2^{nd} order pressure

Figure 9: Vortex decay. Convergence for 3^{rd} order velocity.

Table 7: Vortex decay. Calculated rate of convergence for 3^{rd} order velocity.

Method	Mass Matrix	Velocity	Pressure
EX (1^{st} Order Pressure)	Consistent	3.553	3.528
EX (1^{st} Order Pressure)	Lumped	3.407	3.402
EX (2^{nd} Order Pressure)	Consistent	3.560	3.556
EX (2^{nd} Order Pressure)	Lumped	3.413	3.423

ensure convergence at each time instance. The L2 norm of the velocity and pressure tolerance was chosen to be 10^{-12}. The quasi-implicit scheme conjugate gradient iteration was very insensitive to the chosen tolerance (the residual was normalised to the first value at each time instance). A tolerance of smaller than 10^{-4} produced a solution accurate to at least 4 significant figures.

Although the fully-explicit method seems to be favoured by the use of higher order BDF, the quasi-implicit method has also demonstrated a second order accuracy for the velocity. To complete the assessment of the two approaches, representative run times are presented in Tab. 9.

It is clear that the fully-explicit method has a much higher computational cost. The first order quasi-implicit demonstrates an equivalent magnitude error with better than 1/100th the computational time. For the second order schemes, an equivalent velocity error is achieved with even greater efficiency. This is also true when compared to the third order fully-explicit scheme. Thus, the quasi-implicit scheme demonstrates a significant speed advantage over that of the fully-explicit scheme.

Before concluding, it is worth determining the characteristics of the quasi-implicit and fully-explicit methods on a non-uniform structured mesh (as used in the first benchmark). Examining only the second order pressure quasi-implicit projection method, the rate of convergence of the pressure for the $\boldsymbol{M} + \Delta t \boldsymbol{K}$

Table 8: Vortex decay. Influence of chosen L2 norm tolerance (pressure and velocity) on calculated error and run times for the fully-explicit (consistent mass matrix) 3^{rd} order BDF scheme with 1^{st} order pressure.

Tolerance	Velocity	Pressure	Run Time	Total Iterations
1.00E-04	1.57E-01	9.09E-01	43.35	18200
1.00E-06	2.43E-03	4.29E-02	131.99	55700
1.00E-08	1.12E-03	7.20E-03	221.24	93400
1.00E-10	1.10E-03	5.74E-03	310.86	131400
1.00E-12	1.10E-03	5.72E-03	374.42	169300

Table 9: Vortex decay. Run times and associated L2 norm error for various simulations.

	Mass Matrix	Step 3	Δt	Velocity	Pressure	Run Time
1^{st} Order Velocity / 1^{st} Order Pressure						
QI	Lumped	$\boldsymbol{M}+\Delta t\boldsymbol{K}$	6.25E-03	3.15E-03	3.97E-02	8.66
QI	Consistent	$\boldsymbol{M}+\Delta t\boldsymbol{K}$	6.25E-03	3.03E-03	3.93E-02	8.79
QI	Lumped	$\boldsymbol{M}$	6.25E-03	3.21E-03	1.68E-02	7.77
QI	Consistent	$\boldsymbol{M}$	6.25E-03	3.10E-03	1.68E-02	7.81
EX	Lumped	-	6.25E-03	3.08E-03	1.58E-02	1098.48
EX	Consistent	-	6.25E-03	2.96E-03	1.53E-02	1156.97
2^{nd} Order Velocity / 2^{nd} Order Pressure						
QI	Lumped	$\boldsymbol{M}+\Delta t\boldsymbol{K}$	2.00E-02	2.17E-05	9.58E-02	3.19
QI	Consistent	$\boldsymbol{M}+\Delta t\boldsymbol{K}$	2.00E-02	9.71E-05	9.54E-02	3.18
QI	Lumped	$\boldsymbol{M}$	2.00E-02	1.33E-04	6.79E-02	1.92
QI	Consistent	$\boldsymbol{M}$	2.00E-02	3.20E-04	9.17E-02	2.59
EX	Lumped	-	2.00E-02	2.42E-04	2.52E-03	405.04
EX	Consistent	-	2.00E-02	3.54E-04	2.99E-03	431.69
3^{rd} Order Velocity / 1^{st} Order Pressure						
EX	Lumped	-	6.25E-02	2.92E-04	1.50E-03	418.54
EX	Consistent	-	6.25E-02	1.80E-04	1.15E-03	444.66
3^{rd} Order Velocity / 2^{nd} Order Pressure						
EX	Lumped	-	6.25E-02	2.87E-04	1.49E-03	435.68
EX	Consistent	-	6.25E-02	1.75E-04	1.15E-03	464.83

variant is equivalent. This is replicated for the consistent $\boldsymbol{M}$ matrix variant. However, as previously, the lumped $\boldsymbol{M}$ approach demonstrates a varying rate of convergence. For this mesh, the use of velocity boundary conditions on the stability parameter $\boldsymbol{Z}$, when utilising a lumped mass matrix, is detrimental. Without imposing stability boundary conditions, the error magnitude is reduced for a given time step. If the lumped mass matrix case is excluded due to inconsistent behaviour, then from the results on both meshes (Fig. 10), the behaviour of the $\boldsymbol{M}+\Delta t\boldsymbol{K}$ cases is optimal. The fully explicit method demonstrates rates of convergence in excellent agreement between both meshes.

7 Third Benchmark - Flow around a cylinder at Re=100

While the previous section investigated a transient problem with a uniform mesh, this problem is intended to examine the fully-explicit and quasi-implicit methods on a large unstructured mesh. The problem is a typical benchmark, with a no slip surface on the cylinder and a slip condition imposed on the horizontal walls. A uniform flow is imposed at the inlet and the pressure condition $p = 0$ is imposed at the exit. Initially, all points in the domain experience a uniform horizontal flow. The Reynolds number is defined based upon the diameter of the cylinder (D=1) and the inlet velocity. The width of the domain (30D) has been chosen to negate the influence of the lateral boundaries on the flow downstream of the cylinder (Behr et al. 1995). The cylinder is placed at the horizontal mid-line, at a distance of 15D from the inlet. The whole computational domain length is 35D. The mesh used is given in Fig. 11, it consists of 147246 linear triangular elements with 74559 nodes. Additional refinement is included in the wake region of the cylinder and proximal to the cylinder. The areas of the elements range by six orders of magnitude. Two quad core Intel Nehalem Xeon (3Ghz) processors from a small cluster were used to conduct the simulations.

On the basis of the results obtained for the previous benchmarks, the third order fully-explicit method is used, together with the second order (pressure and velocity) quasi-implicit scheme. Since the third order BDF is not 'self-starting', an adaptive procedure is implemented, with a first order BDF for the first time step, and a second order BDF for the second time step. The quasi-implicit scheme used the $\boldsymbol{M}+\Delta t\boldsymbol{K}$ matrix both within the pressure and correction steps. The explicit and quasi implicit schemes employed a real time step of 0.16666666 and 0.001302083, respectively. The simulation was run until a non-dimensional time of 166.66. The average mass imbalance at the inlet and exit was determined as 0.03% when imposing velocity boundary conditions upon the stability variable $\boldsymbol{Z}$ within the quasi-implicit scheme. Without these boundary conditions, the average mass imbalance was negligible (0.0003%). Due to the negative impact on convergence detailed in the previous section and because of the mass imbalance, the following results were

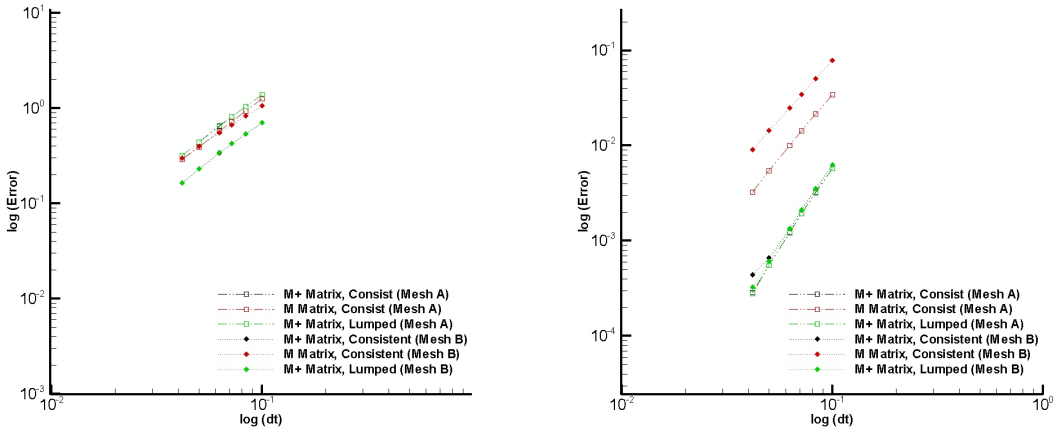

(a) Pressure

(b) Velocity

Figure 10: Vortex decay. Convergence on Mesh A and Mesh B using the quasi-implicit projection method.

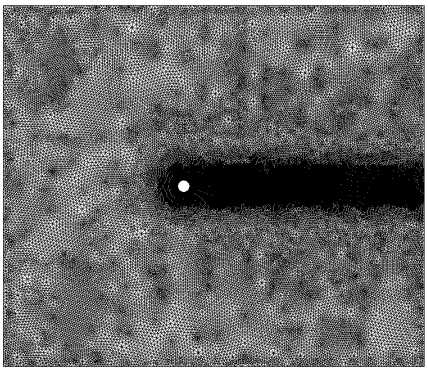

Figure 11: Flow around a cylinder. Unstructured mesh.

Table 10: Flow around a cylinder. Predicted flow properties.

Method	Mass Matrix	Strouhal Number	C_{lift}	C_{Drag}	Run time (s)
QI	Consistent	0.1670	0.332	1.356	21286.1
EX	Consistent	0.1666	0.332	1.356	144089.6
QI	Lumped	0.1665	0.346	1.361	22565.4
EX	Lumped	0.1660	0.346	1.360	139499.5

not obtained using velocity boundary conditions on the stability variable. The distributions of the velocity and pressure at the non-dimensional time of 150 are given in Fig. 12.

The results are in good qualitative agreement, although minor differences exist. This is likely due to the fully-explicit scheme requiring a relatively small convergence tolerance. A normalised velocity error was employed with a convergence tolerance of 10^{-5}. The computational cost would increase significantly if the tolerance is decreased.

The calculated coefficients of drag and lift are depicted in Fig. 13. The phase of the vortex shedding is marginally different in all cases, and the choice of lumped or consistent mass matrix does have a small impact on the lift and drag coefficients once shedding has started. The predicted amplitudes of drag and lift coefficients are in excellent agreement for both schemes.

The predicted Strouhal number, along with the coefficients of lift and drag, are given in Tab. 10 for both methods. The Strouhal number was calculated using the vertical velocity at point [11.0,0.0]. From the results, the quasi-implicit method is marginally more accurate over both cases in predicting the Strouhal number (0.1667), with an average error of 0.05% compared to the fully-explicit error of 0.21%. The run time of the quasi-implicit method is also significantly faster (6.77x using consistent mass matrix) than the fully-explicit scheme. The maximum mass imbalance for the fully-explicit method was 0.084%, while for the quasi-implicit method it was 0.004%. A smaller tolerance would greatly increase the cost of the fully-explicit method.

Results examining the use of velocity boundary conditions for the intermediate velocity field are presented in Fig. 14 for the quasi-implicit method. There is no impact on the fully-explicit method, as noted earlier, and only a very small impact when using the quasi-implicit method. This takes the form of a minor phase difference in the vortex shedding, rather than in the predicted Strouhal number or drag coefficient. For the fully-explicit method, the lack of impact extends to both the number of iterations and the predicted results. The use of boundary conditions does have one relatively major impact on the number of iterations required within the quasi-implicit method, being reduced by 10.1% and 19.3% for the consistent and lumped mass matrix cases respectively. The difference between the consistent and lumped variants is due to the lumped mass matrix (without intermediate velocity boundary conditions) undertaking 8.9% more iterations than the comparable consistent mass matrix case. When intermediate boundary conditions are employed, the difference between the lumped and consistent mass matrix iterations is negligible. Since the results are in excellent agreement, and noting that both contain identified sources of error, the use of intermediate velocity boundary conditions is desirable due to the reduced computational cost.

8 Concluding Remarks

In this paper, we reviewed some of the classical aspects of fractional step methods, in reference to the CBS scheme. In particular, three principal forms of the scheme have been investigated and compared, with a variant of the quasi-implicit scheme. The quasi-implicit method possess a significant speed advantage (from 3-100x) over the fully-explicit approach. The semi-implicit method is inferior to the quasi-implicit, due to the additional stability criteria imposed by the diffusive component within the momentum equations.

Second order pressure split appears unnecessary for the fully-explicit scheme, due to the use of artificial compressibility. This requires a pseudo timestepping iterative mechanism, which removes the pressure order of convergence from the true transient properties of the scheme. As such, the use of second order and higher BDF for the velocity results in the pressure also displaying an equivalent rate of convergence. The use of a second order pressure projection does however improve the convergence of the quasi-implicit scheme.

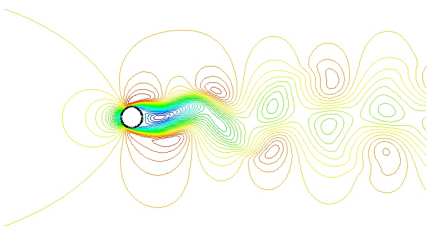

(a) QI, u

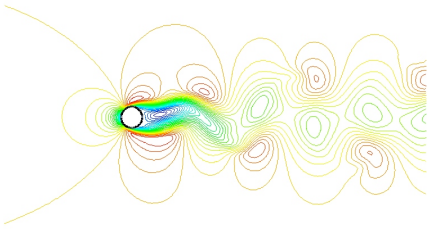

(b) EX, u

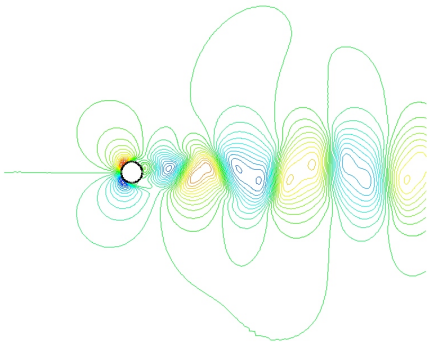

(c) QI, v

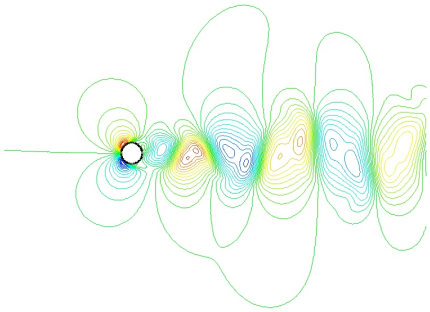

(d) EX, v

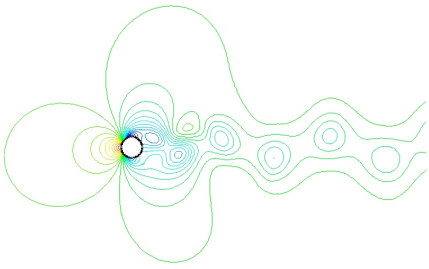

(e) QI, p

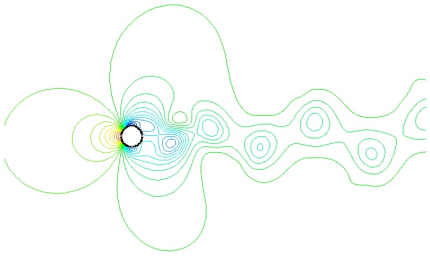

(f) EX, p

Figure 12: Flow around a cylinder. Contours of the velocity and pressure as predicted by the fully-explicit method and the quasi-implicit scheme for a selected region of the domain at $t = 150$ and using a consistent mass matrix.

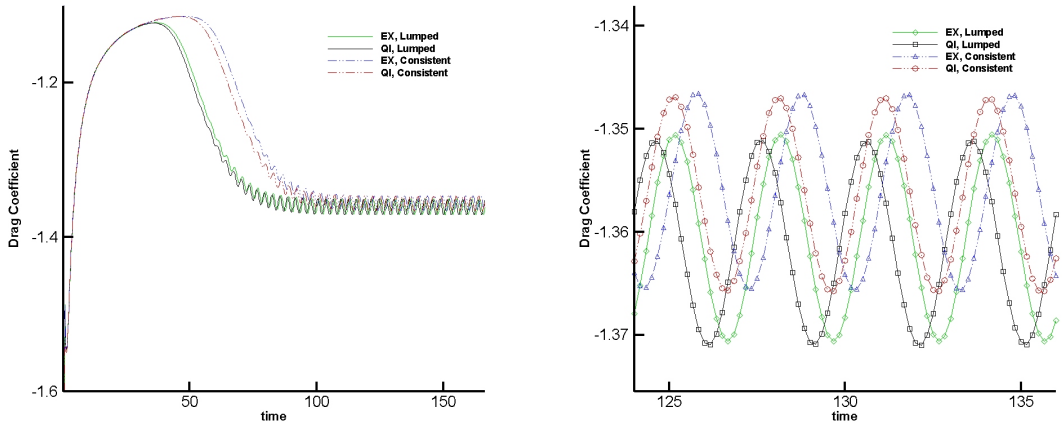

(a) Drag (b) Drag

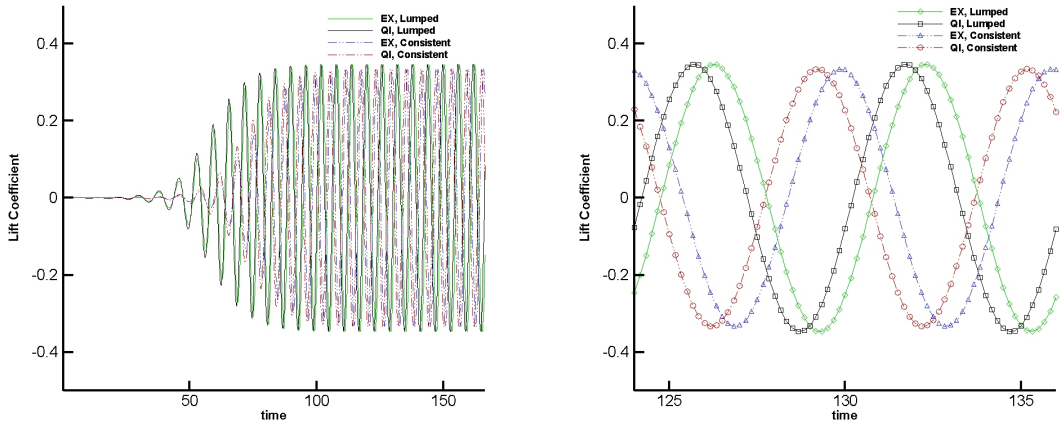

(c) Lift (d) Lift

Figure 13: Flow around a cylinder. Comparison between the calculated coefficients of drag and lift.

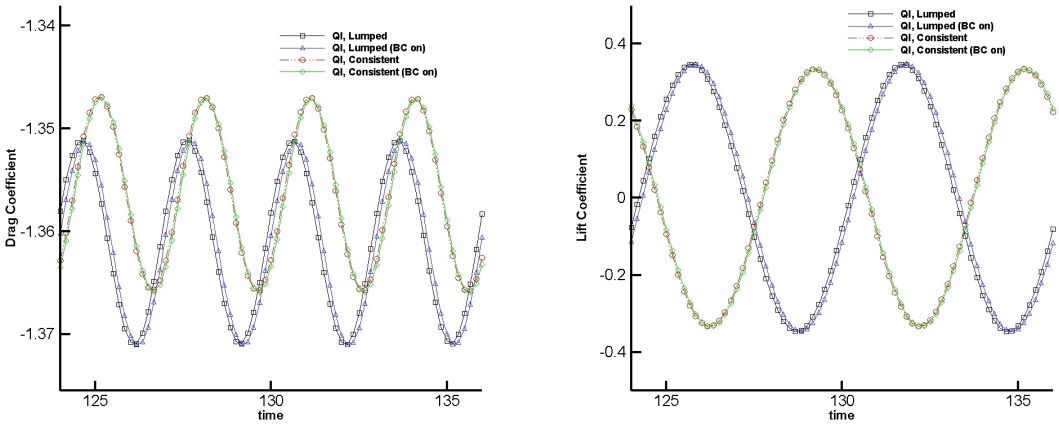

(a) Drag

(b) Lift

Figure 14: Flow around a cylinder. Impact of intermediate velocity boundary conditions on the drag and lift coefficients.

The results of the second benchmark demonstrate that the velocity error is decreased when the second variant of the quasi-implicit method is used, with Eqn. (14). This has negligible impact on the computational cost of the scheme.

Imposition of boundary conditions was examined for the intermediate velocity $\boldsymbol{u}_i^*$ and the stability variable $\boldsymbol{Z}$. In the later case, this has a positive impact on the convergence and instantaneous error for the lumped mass matrix quasi-implicit scheme. When the diffusive component is included within the matrix of the correction step, however, there is a negative impact on the rate of convergence of both velocity and pressure. The instantaneous pressure error is reduced, although this is not necessarily true of the velocity. As for imposing velocity boundary conditions on the intermediate velocity field, this is of benefit in circumstances where the pressure gradient at the boundary is nearly zero. This is due to the error imposed while calculating the edge diffusive component using linear elements.

The use of a lumped or consistent mass matrix had little impact on the computational cost of either the fully-explicit or the quasi-implicit schemes. This was also true of the influence on accuracy, compared to the analytical solution of the vortex decay benchmark. A small effect on the convergence was noted for small time step values, with a lumped mass matrix being of a marginally better value in some cases, but not for the third order fully-explicit solution. While the impact is stronger for the benchmark problem of flow around a cylinder at Re=100, the calculated Strouhal number and coefficients of drag and lift are in relatively good agreement.

The quasi-implicit projection method presented in this work has demonstrated its suitability on both structured and unstructured meshes. While a global time step is necessary, not even an element area range of six orders of magnitude has prevented the quasi-implicit method from being a faster numerical method to that of the artificial compressibility-based fully-explicit method. The quasi-implicit method's computational cost would be further reduced with the use of an improved preconditioner for the conjugate gradient solver.

References

Armfield, S. & Street, R. (2002), 'An analysis and comparison of the time accuracy of fractional-step methods for the navierstokes equations on staggered grid', *Int. J. Numer. Meth. Fl.* **38**, 255–282.

Arpino, F., Massarotti, N. & Mauro, A. (2010), 'A stable explicit fractional step procedure for the solution

of heat and fluid flow through interfaces between saturated porous media and free fluids in presence of high source terms', *Int. J. Numer. Meth. Eng.* **83**, 671–692.

Behr, M., Hastreiter, D., Mittal, S. & Tezduyar, T. (1995), 'Incompressible flow past a circular cylinder: dependence of the computed flow field on the location of the lateral boundaries', *Comput. Method Appl. M.* **123**, 309–316.

Bell, J., Colella, P. & Glaz, H. (1989), 'A second order projection method for the incompressible navierstokes equations', *J. Comput. Phys.* **85**, 257–283.

Bevan, R., Nithiarasu, P., Loon, R. V., Sazonov, I., Luckraz, H. & Garnham, A. (2010), 'Application of a locally conservative Galerkin (LCG) method for modelling blood flow through a patient-specific carotid bifurcation', *Int. J. Numer. Meth. Fl.* **64**, 1274–1295.

Bevan, R., Sazonov, I., Saksono, P., Nithiarasu, P., Loon, R. V., Luckraz, H. & Ashraf, S. (2011), 'Patient-specific blood flow simulation through an aneurysmal thoracic aorta with a folded proximal neck', *Int. J. Numer. Method Biomed. Eng.* **27**, 1167–1184.

Blasco, J., Codina, R. & Huerta, A. (1998), 'A fractional-step method for the incompressible Navier-Stokes equations related to a predictor-multicorrector algorithm', *Int. J. Numer. Meth. Fl.* **28**, 1391–1419.

Brown, D. L., Cortez, R. & Minion, M. L. (2001), 'Accurate projection methods for the incompressible Navier-Stokes equations', *J. Comput. Phys.* **168**, 464–499.

Burton, T. M. & Eaton, J. K. (2002), 'Analysis of a fractional-step method on overset grids', *J. Comput. Phys.* **177**, 336–364.

Chang, W., Giraldo, F. & Perot, B. (2002*a*), 'Analysis of an exact fractional step method', *J. Comput. Phys.* **180**, 183–199.

Chang, W., Giraldo, F. & Perot, B. (2002*b*), 'Analysis of an exact fractional step method', *J. Comput. Phys.* **180**(1), 183–199.

Chorin, A. (1968), 'Numerical solution of the Navier-Stokes equations', *Math. Comput.* **22**(104), 745–762.

Chorin, A. (1969), 'On the convergence of discrete approximation to the Navier-Stokes equations', *Math. Comput.* **23**, 341–353.

Codina, R. (2001), 'Pressure stability in fractional step finite element methods for incompressible flows', *J. Comput. Phys.* **170**, 112–140.

Codina, R. & Blasco, J. (1997), 'A finite element formulation for the stokes problem allowing equal velocity-pressure interpolation', *Comput. Method Appl. M.* **143**, 373–391.

Codina, R., Coppola-Owen, H., Nithiarasu, P. & Liu, C.-B. (2006), 'Numerical comparison of CBS and SGS as stabilization techniques for the incompressible Navier-Stokes equations', *Int. J. Numer. Meth. Eng.* **66**, 1672–1689.

Codina, R., Vázquez, M. & Zienkiewicz, O. (1998), 'A general algorithm for compressible and incompressible flows. part III: The semi-implicit form', *Int. J. Numer. Meth. Fl.* **27**, 13–32.

deSampaio, P. A. B., Lyra, P. R. M., Morgan, K. & Weatherill, N. P. (1992), 'Petrov galerkin solutions of the incompressible navier-stokes equation in primitive variables with adaptive remeshing', *Comput. Method Appl. M.* **106**, 143–178.

Drikakis, D., Govatsos, P. A. & Papantonis, D. E. (1994), 'A characteristic-based method for incompressible flows', *Int. J. Numer. Meth. Fl.* **19**, 667–685.

Dukovicz, J. & Dvinsky, A. (1992), 'Approximate factorization as a high-order splitting for the implicit incompressible flow equations', *J. Comput. Phys.* **102**, 336–347.

Ghia, U., Ghia, K. N. & Shin, C. T. (1982), 'High-re solutions for incompressible flow using the navier-stokes equations and a multigrid method', *J. Comput. Phys.* **48**, 387 – 411.

Gresho, P. M., Lee, R. L., Sani, R. L., Maslanik, M. K. & Eaton, B. E. (1987), 'The consistent galerkin fem for computing derived boundary quantities in thermal and/or fluids problems', *Int. J. Numer. Meth. Fl.* **7**, 371–394.

Guermond, J. & Shen, J. (2003*a*), 'A new class of truly consistent splitting schemes for incompressible flows', *J. Comput. Phys.* **192**, 26–276.

Guermond, J. & Shen, J. (2003*b*), 'Velocity-correction projection methods for incompressible flows', *SIAM J. Numer. Anal.* **41**(1), 112–134.

Kim, J. & Moin, P. (1985), 'Application of a fractional-step method to incompressible Navier-Stokes equations', *J. Comput. Phys.* **59**, 308–323.

Lee, M., Oh, B. D. & Kim, Y. (2001), 'Canonical fractional-step methods and consistent boundary conditions for the incompressible navierstokes equations', *J. Comput. Phys.* **168**, 73–100.

Li, X. & Duan, Q. (2006), 'Meshfree iterative stabilized Taylor-Galerkin and characteristic-based split (CBS) algorithms for incompressible N-S equations', *Comput. Method Appl. M.* **195**, 6125–6145.

Massarotti, N., Arpino, F., Lewis, R. W. & Nithiarasu, P. (2006), 'Explicit and semi-implicit CBS procedures for incompressible viscous flows', *Int. J. Numer. Meth. Eng.* **66**, 1618–1640.

Morandi-Cecchi, M. & Venturin, M. (2006), 'Characteristic-based split (CBS) algorithm finite element modelling for shallow waters in the venice lagoon', *Int. J. Numer. Meth. Eng.* **66**, 1641–1657.

Nithiarasu, P. (2002), 'On boundary conditions of the characteristic based split (cbs) algorithm for fluid dynamics', *Int. J. Numer. Meth. Eng.* **54**, 523–536.

Nithiarasu, P. (2003), 'An efficient artificial compressibility (AC) scheme based on the charcteristic based split (CBS) method for incompressible flows', *Int. J. Numer. Meth. Eng.* **56**, 1815–1845.

Nithiarasu, P. (2004), 'A simple locally conservative Galerkin (LCG) finite element method for transient conservation equations', *Numerical Heat Transfer, Part B Fundamentals* **46**, 357–370.

Nithiarasu, P., Codina, R. & Zienkiewicz, O. C. (2006), 'The characteristic based split scheme - a unified approach to fluid dynamics', *Int. J. Numer. Meth. Eng.* **66**, 1514–1546.

Nithiarasu, P., Hassan, O., Morgan, K., Weatherill, N. P., Fielder, C., Whittet, H., Ebden, P. & Lewis, K. R. (2008), 'Steady flow through a realistic human upper airway geometry', *Int. J. Numer. Meth. Fl.* **57**, 631–651.

Nithiarasu, P., Mathur, J. S., Weatherill, N. P. & Morgan, K. (2004), 'Three dimensional incompressible flow calculations using the characteristic based split (CBS) scheme', *Int. J. Numer. Meth. Fl.* **44**, 1207–1229.

Nithiarasu, P. & O.C.Zienkiewicz (2000), 'On stabilization of the CBS algorithm. internal and external time steps', *Int. J. Numer. Meth. Eng.* **48**, 875–880.

Nithiarasu, P. & Zienkiewicz, O. C. (2006), 'Analysis of an explicit and matrix free fractional step method for incompressible flows', *Comput. Method Appl. M.* **195**, 5537 – 5551.

Perot, J. B. (1993), 'An analysis of the fractional step method', *J. Comput. Phys.* **108**, 51–58.

Shen, J. (1992), 'On error estimates of projection methods for Navier-Stokes equations: First order schemes', *SIAM J. Numer. Anal.* **29**, 57–77.

Strikwerda, J. C. & Lee, Y. S. (2000), 'The accuracy of the fractional step method', *SIAM J. Numer. Anal.* **37**(1), 37–47.

Temam, R. (1977), *Navier-Stokes equations. Theory and numerical analysis*, North-Holland, Amsterdam.

Temam, R. (1991), 'Remark on the pressure boundary condition for the projection method', *Theor. Comput. Fluid Dyn.* **3**, 181–184.

Temam, R. (n.d.), 'Sur l'approximation de la solution des équations de Navier-Stokes par la méthode des pas fractionaires', *Arch. Rat. Mech. Anal.* **32**.

Thomas, C. G., Nithiarasu, P. & Bevan, R. L. T. (2008), 'The locally conservative Galerkin (LCG) method for solving incompressible Navier-Stokes equations', *Int. J. Numer. Meth. Fl.* **57**, 1771–1792.

van Kan, J. (1986), 'A second-order accurate pressure-correction scheme for viscous incompressible flow', *SIAM J. Sci. Comput.* **7**(3), 870–891.

Zienkiewicz, O. C. & Codina, R. (1995), 'A general algorithm for compressible flow and incompressible flow - part I. the split characteristic-based scheme', *Int. J. Numer. Meth. Fl.* **20**, 869–885.

Zienkiewicz, O. C., Morgan, K., Sai, B. V. K. S., Codina, R. & Vazquez, M. (1995), 'A general algorithm for compressible flow - part II. tests on the explicit form', *Int. J. Numer. Meth. Fl.* **20**, 887–913.

Zienkiewicz, O. C., Taylor, R. L. & Nithiarasu, P. (2005), *The finite element method for fluid Dynamics*, Elsevier Butterworth Heinemann, London.